Environ Earth Sci (2016)75:154
DOI 10.1007/s12665-015-4891-8

ORIGINAL ARTICLE

Submarine groundwater discharge as a source of dissolved nutrients to an arid coastal embayment (La Paz, Mexico)

Mabilia Urquidi-Gaume[1] · Isaac R. Santos[2] · Carlos Lechuga-Deveze[1]

Received: 15 February 2015 / Accepted: 3 August 2015

Abstract Submarine groundwater discharge (SGD) was investigated in the southeastern portion of La Paz Bay (Baja California, Mexico) using radon (^{222}Rn) as a natural tracer. In the absence of permanent surface flows in this arid region, we hypothesize SGD is a major regional source of dissolved nutrients. Four spatial surveys showed higher radon and nutrient (NH_4, NO_3, NO_2, PO_4 and SiO_4) values in the winter than summer lagging rainfall by 3–4 months. The surveys revealed two sites (Balandra and Merito) with a stronger radon signal. Intensive time series (12–24 h) measurements at those sites were used to estimate SGD fluxes using a radon mass balance approach. In Balandra, SGD was estimated to be 0.18 m^3 m^{-2} day^{-1} and significant correlations between radon and nutrients (NO_3 and SiO_4) were observed. In Merito, SGD rates were estimated to be 0.10 m^3 m^{-2} day^{-1} and no correlations between nutrients and ^{222}Rn were observed. The difference between the two sites was interpreted to be related to different components dominating SGD (i.e., fresh SGD in Balandra and saline SGD in Merito). The estimated SGD-derived nutrients fluxes were 2–52, 0.04–0.94, 7–164 mmol m^2 day^{-1} for dissolved inorganic nitrogen, phosphate, and silicate, respectively. These fluxes could explain between 5 and 20 % of the regional marine primary productivity values.

Keywords Submarine groundwater discharge · Coastal aquifer · ^{222}Rn · Arid coast · Isotopic tracers · Coastal biogeochemistry

Introduction

Submarine groundwater discharge (SGD) has been recognized as an important pathway delivering water and solutes from land to sea (Burnett et al. 2003; Moore 2010). SGD may play a significant ecological role in spite of the small water volume because nutrient concentrations in groundwater are usually significantly higher than the receiving coastal waters (Slomp and Van Cappellen 2004). In some cases, dissolved nutrients such as nitrogen, phosphorus and silica associated with SGD fluxes can account for a large fraction of the nutrients delivered by regional rivers (Johannes 1980; Kroeger and Charette 2008; Niencheski et al. 2007; Santos et al. 2014). As a result, SGD may be associated with highly productive coastal communities (Herrera-Silveira 1998; Hwang et al. 2005; Waska and Kim 2010) and influence the trophic status of coastal waters (Valiela et al. 1990).

In a broad sense, SGD can be understood as any flux of water from marine sediments to the water column. Hence, SGD is often made up of a mixture of freshwater and recirculated marine water (Burnett et al. 2003). SGD dynamics has been investigated using different natural tracers (Burnett et al. 2006). Using radon (^{222}Rn) as a tracer has been found to be an effective method for mapping and quantifying SGD due to its conservative behavior, natural occurrence in rocks and soils, and high concentration in groundwater in comparison to surface waters (Burnett et al. 2006; Schmidt et al. 2008). In addition, radon has a short half-life time ($t_{1/2} = 3.84$ days) that is comparable to

✉ Mabilia Urquidi-Gaume
ocean.mysteries@gmail.com

[1] Centro de Investigaciones Biológicas del Noroeste (CIBNOR), Mar Bermejo 195, Colonia Playa Palo de Santa Rita, 23096 La Paz, B.C.S., Mexico

[2] National Marine Science Centre, School of Environment, Science and Engineering, Southern Cross University, Coffs Harbour, NSW 2450, Australia

Published online: 06 January 2016

residence times in many coastal systems. These characteristics allow the identification of points of discharge in surface waters (Santos et al. 2012a; Stieglitz et al. 2010). Continuous measurement of ^{222}Rn allows the construction of mass balances from which quantitative estimates of groundwater discharge can be obtained (Burnett and Dulaiova 2003; Perkins et al. 2015; Santos et al. 2015).

Only a few studies on SGD and its biogeochemical implications have been performed in arid coasts where rainfall is very low, evaporation is high and only ephemeral rivers discharge freshwater to the ocean. For example, while SGD contributed only to 1–2 % of the water to the Gulf of Aqaba (Israel), it accounted for 8–46 % of regional dissolved nutrient budgets (Shellenbarger et al. 2006). Very few studies have used geochemical tracers to assess SGD in Mexico, and most of them focus on the Yucatan Peninsula, a karstic system with high rainfall rates (Aranda-Cirerol et al. 2006; Young et al. 2008). Santos et al. (2011) investigated SGD associated with hydrothermal vents in Concepción Bay, an arid embayment in the Baja California Peninsula. This work revealed that new nitrogen inputs associated with hydrothermal inputs accounted for at least 15 % of the new local primary productivity, but the estimates were considered conservative.

Arid embayments may behave as inverse estuaries in which evaporation is greater than freshwater inputs, resulting in higher salinities towards the head of these systems (Largier et al. 1997). Increased salinities may enhance surface water densities, driving convective pore water exchange at the sediment water interface (Santos et al. 2012b). Assessing SGD in arid regions is important because other sources (i.e., river inputs) are restricted, potentially enhancing the relative contribution of SGD to coastal nutrient budgets. In spite of low rainfall rates, fractured sedimentary or volcanic rocks in arid and semi-arid zones may act as effective groundwater conduits (Swarzenski et al. 2006; Weinstein et al. 2007). In this paper, we assess SGD along the southern portion (30 km) coast of La Paz Bay (Baja California, Mexico), an inverse estuary arid embayment surrounded by fractured rocks. Our specific objectives were: (1) to identify sites where SGD is occurring using a radon survey approach, (2) to quantify SGD fluxes using a radon mass balance, and (3) to estimate SGD-derived nutrient fluxes.

Study site

This study was conducted in La Paz Bay, in the southeastern coast of the Baja California Península, México (Fig. 1). La Paz Bay is characterized by mixed semidiurnal tides. The bay is up to 450-m deep in the north and shallower towards the southeastern part (∼10 m) (Cruz-Orozco et al. 1996). The zone is characterized by an arid climate. Summer maximum temperatures are 36–40 °C, annual average rainfall is only ∼200 mm and annual evaporation rate is of 2000–2200 mm. Most of the annual rainfall occurs during summer associated with storms and hurricane events. Rivers are ungauged and ephemeral following these events (Mendoza-Salgado et al. 2006).

The southeastern portion La Paz Bay consists of small coastal lagoons with mangrove communities, a series of coves with pocket beaches and sometimes small dunes formed between low headlands of volcanic origin (Velasco-García 2009). This study focused on two of those embayments (Balandra and Merito, Fig. 1). Balandra is a cove 720-m wide and 1150-m long and 0.5-m to 25-m deep. Merito is a cove with a pocket beach in the head. Merito has a small slope in the beach face area, and maximum depths of 3 with a small fringing mangrove community. Both Merito and Balandra are undisturbed by human activities.

These embayments are located in transitional area between two geologic and physiographic regions, La region del Cabo and the La Region Sierra de la Giganta. These regions are separated by a system of faults and grabens known as "La Paz Valley" and "Coyote Valley" (Sedlock et al. 1993). The coastal area constitutes a narrow fringe of land on the northwest-facing slope of sedimentary deposits described as free aquifers within a heterogenous lithological system. The sedimentary deposits overlay a basement of granitic rock (cretaceous) in contact with sequences of volcano–sedimentary rocks (sandstones, clays, and volcanic conglomerate) and deposits of alluvium (Aranda-Gómez 1982). The aquifer of the Coyote Valley has been described as having 4 units: (1) a shallow unit with conglomerates and a sandy-clay matrix (100–250 m deep); (2) a unit conformed of non-consolidated materials (sands, clays, gravel) which constitutes the aquifer; (3) a very low permeable unit made up of sandstones and clays; (4) and granite basement. The intense faulting and fracturing on rocks for this region create secondary permeability, which allows rain to be transmitted through the cracks afterwards being gradually released in low-lying area as springs (Chávez-López 2010).

Methods

Spatial surveys measuring radon activity were carried to map potential SGD hotspots in the southern portion of La Paz Bay. Four surveys were carried during neap tide conditions on a similar path (09 Dec 2009, 05 Feb 2010, 21 April 2010, and 18 June 2010) along 30 km of coastline (Fig. 1). Hereafter, these surveys are referred to as R1, R2, R3 and R4, respectively. Radon activity was measured with

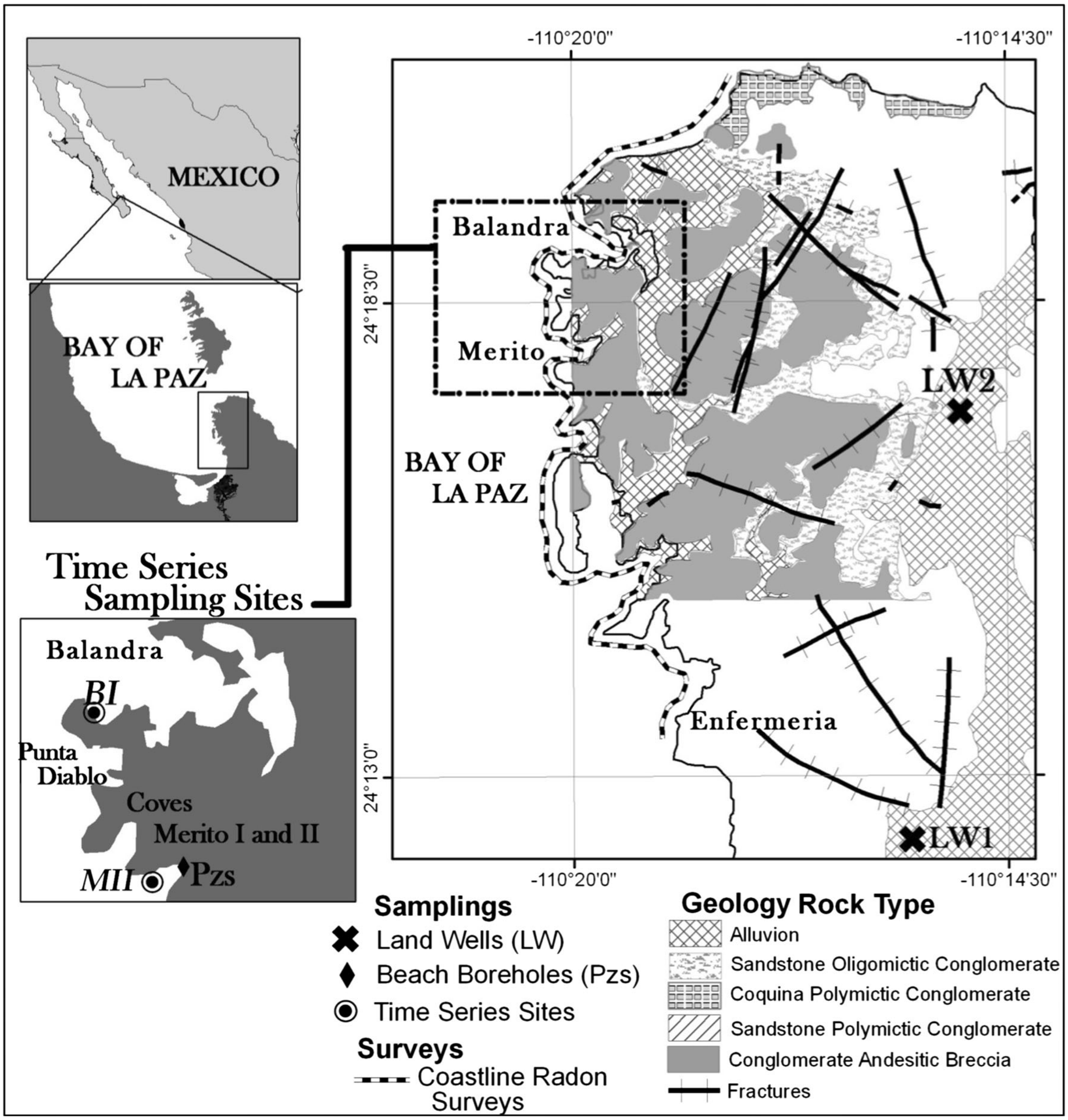

Fig. 1 The location of the study site in Mexico

an automated radon detector (RAD7-Durridge, Co., Inc.) from a moving boat at about 5 km/hr similar to previous studies (Dulaiova et al. 2005; Macklin et al. 2014; Stieglitz et al. 2010). Surface water (0.5 m below the surface) was continuously pumped to an air–water equilibrium chamber that degassed radon. Radon in water equilibrated with radon in the air and then it was measured by the RAD7. The ^{222}Rn activities were integrated every 15 min after corrections that rely on temperature and salinity observations (Schubert et al. 2012). Water temperature and conductivity were measured with an YSI multi-parameter probe (model 6117) and Van Essen Data Divers (model DI-263). Nutrient (nitrate—NO_3, nitrite—NO_2, ammonium—NH_4, ortho-phosphate—PO_4, and silicate—SiO_4) samples were taken every ~1 km, filtered with disposable 0.45-μm filters, and frozen for later analysis. Nutrient analysis was carried out at CIBNOR laboratories using a Lachat QuickChem FIA (Flow Injection Analyzer) following standard procedures (Strickland and Parsons 1972).

Spatial patterns of ^{222}Rn activities' results were mapped in ArcGIS to visualize and select sites with the strongest SGD signal to carry out intensive time series measurements during complete tidal cycles (12–24 h). A total of two sites were selected (Fig. 1). A 24-h time series measurement was done at Merito (24°18′04.38″N, 110°19′39.23″W) along the coast on 18 March 2011 (early spring). A 12-h time series measurement was performed at a small basin called Balandra (24°18′59.85″N, 110°20′10.41″W) in late summer (26 of August 2010). Merito was set in a shallow beach face area (−2 m) with fine-to-coarse sands. Sediments from Merito were completely exposed during low tides. Balandra was set 850 m off the beach face area (with depths up to 4 m), near the mouth of the basin of the coastal lagoon (Fig. 1). Calibrated Van Essen CTD Divers were deployed during the time series experiments to measure depths, temperature, and conductivity. Nutrient samples were taken every hour in the same fashion as during surveys.

Groundwater samples were taken from three wells hand augered at the intertidal zone at different depths (50, 70 and 130 cm) (hereafter "Pzs" for piezometer) and from two local water supply bores located about 10 km onshore (hereafter "LW" for land well). Water samples were taken for radon, temperature and conductivity, and nutrients.

Samples for ^{226}Ra (^{222}Rn parent) were collected in three sites during the 30 km survey (Balandra, Merito and Enfermería). Radium-226 sampling was achieved by pumping 200 L of seawater slowly (1 L min^{-1}) through columns containing Mn impregnated acrylic fiber. In the laboratory, the fibers were prepared and left in a sealed air-tight cartridge for radioactive ingrowth of ^{222}Rn and then counted in a Radium Delayed Coincidence Counting (RaDeCC) following Peterson et al. (2009) and Waska et al. (2008). The ^{226}Ra concentrations were used simply to support the ^{222}Rn interpretation as we do not have enough information to construct a radium mass balance.

The ^{222}Rn observations were used to construct a mass balance to estimate SGD as described in detail by Burnett and Dulaiova (2003). The model is based on the temporal change of ^{222}Rn inventories making allowances for losses due to atmospheric evasion, radioactive decay, and mixing with lower concentration waters offshore. The unaccounted for changes in ^{222}Rn fluxes was assigned to SGD inputs under the assumption that diffusive fluxes were negligible. The SGD fluxes were calculated by dividing the estimated total ^{222}Rn fluxes by the concentration in the advecting fluids. Two scenarios of modeling were taken into account: (1) using the ^{222}Rn borehole data as an end-member for the groundwater fluid and (2) using the land wells groundwater data as an end-member. Wind speed data were obtained from local weather stations to estimate radon evasion to the atmosphere following Burnett and Dulaiova (2003) and references therein.

Results and discussion

Spatial surveys

Radon ranged from 0.4 to 4.2 dpm L^{-1} during the four spatial surveys (Fig. 2). The average NO_3, PO_4 and SiO_4

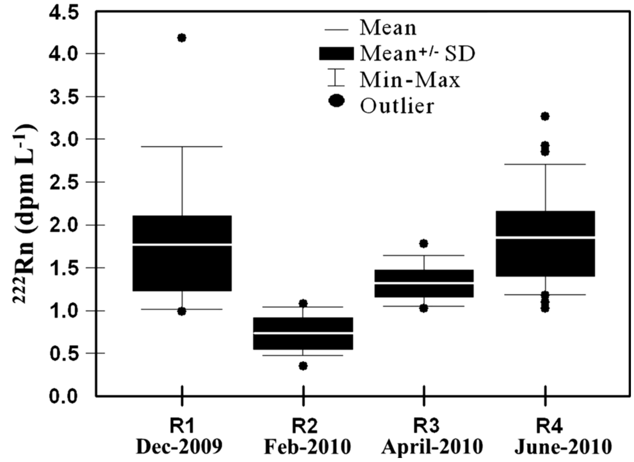

Fig. 2 Radon activities during the four surveys

concentrations were slightly higher in December 2009 and June 2010 coinciding with the highest ^{222}Rn activities (Fig. 3). Nitrite was below detection in most samples (data not shown). Ammonium values were usually higher during R2 when nitrate and radon were the lowest (Fig. 3).

The overall average ^{222}Rn activity during all the surveys was 1.5 dpm L^{-1}, well above the supported ^{226}Ra concentrations of 0.13 dpm L^{-1} (average ^{226}Ra from three sites). Overall, ^{222}Rn values were found comparable to other studies reported in similar arid or semi-arid setting (Table 1). Locations with activities above ~2 dpm L^{-1} are emphasized in Fig. 4 as potential SGD hotspots. Although there was no significant correlation between nutrients and ^{222}Rn in any survey (not shown), they followed a similar pattern showing high values for silicates and nitrates in the same general area of radon enrichment (Fig. 4). The lack of correlation may be related to a lag of ~30 min associated with the radon system used here (Stieglitz et al. 2010), which may prevent a straight forward assessment of spatial correlations.

The highest radon and nutrient values were found in the winter (December 2009) 3.5 months after the main rainfall events (total of 100 mm in September). Therefore, these results are in line with the suggestion that the inland seasonal hydrological cycle and SGD are tightly connected (Michael et al. 2005). The peak SGD may lag 1–5 months behind peak aquifer recharge in Waquoit Bay (USA). The lag in SGD implied from the radon observations is further supported by an additional 37 mm of rainfall between December and February 2009. This rainfall event could explain a minor increase in radon and nutrients during R4 (June 2010; Figs. 2, 3). Related work suggesting an SGD lag were conducted in non-arid areas where water recharge occurs during winter rainfall events and SGD peaks during the summer (Kelly and Moran 2002), or where rainfall occurs in summer and SGD peaks in winter (Moore 1997).

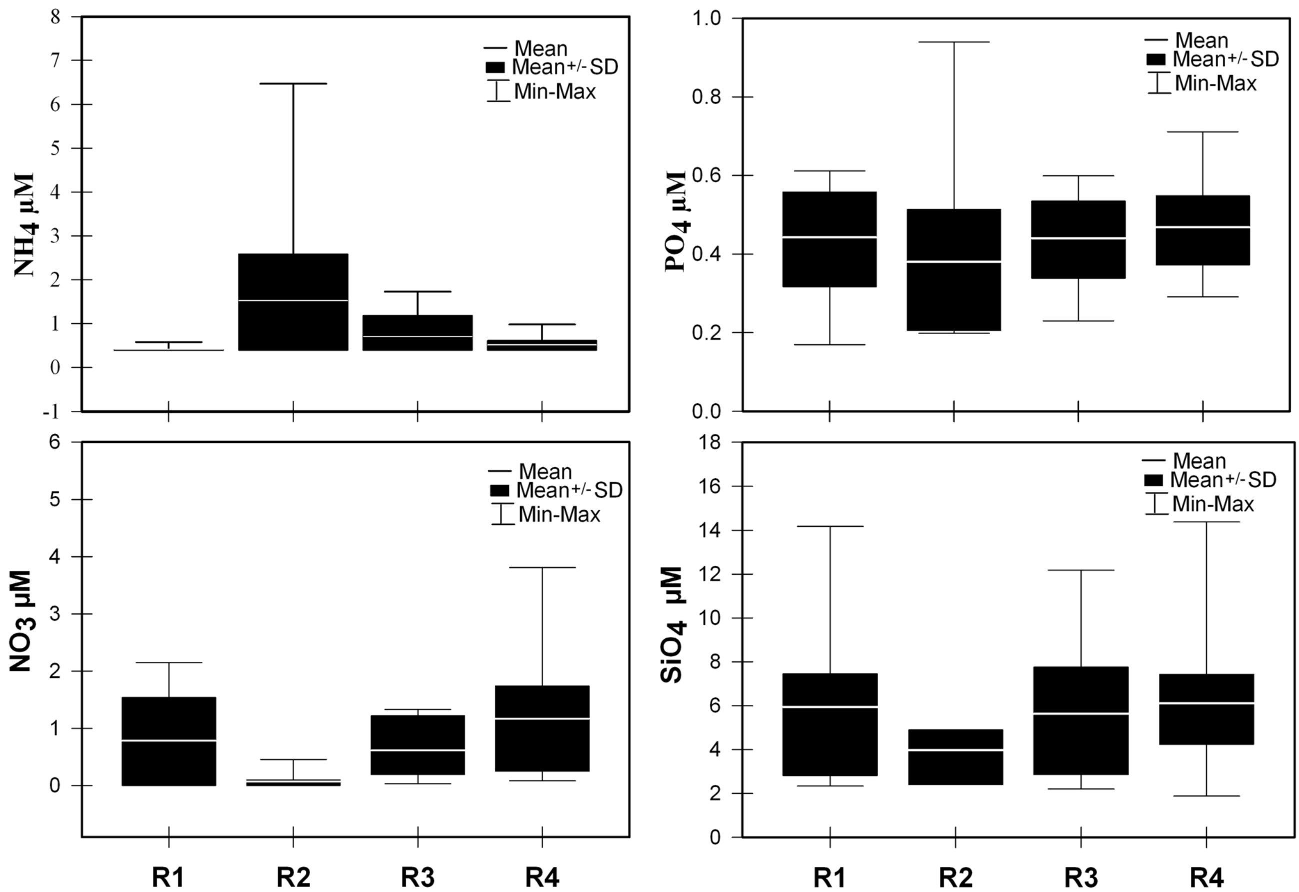

Fig. 3 Nutrient concentration during the four surveys. NO_2 was below detection limit in most cases

Table 1 ^{222}Rn values (dpm L^{-1}) in arid and semi-arid zones

Site	Geology	$^{222}Rn^a$	Distance (m)	^{222}Rn PZP	^{222}Rn LW	References
La Paz Bay, Mexico	Alluvium, and Sandstone Conglomerate with fractures	0.2–4.2	<500	25–34	367–512	This study
Concepcion Bay, Mexico	Volcanic and sedimentary rocks with a fault system. Hydrothermal spring	0.5–3.3	<100	10–23	85–486	Santos et al. (2011)
Dor Bay, Israel	Calcareous Sandstone with fractures, unconsolidated sands	0.1–6.5	<100	19–50	300-425	Swarzenski et al. (2006)
St. Vincent Gulf, Australia	Alluvium, Limestone and Quartz rocks	0.3–0.5	<500	35.4–126	354–1440	Lamontagne et al. (2008)

Distance refers to the distance from the beach face where the surface water ^{222}Rn was measured

PZP shallow piezometers or seepage meters, *LW* onshore freshwater wells

[a] Surface water

Time series

The spatial survey observations allowed us to select two sites for time series experiments: Balandra (August) and Merito (March). Those sites are located at opposite sides of the Punta Diablo headland (260 m high) and had radon values above 3 dpm L^{-1} in at least two spatial surveys (Fig. 4). The average concentrations obtained at the two time series stations are shown in Table 2.

In Merito, higher radon values were observed at low tide (Fig. 5) with positive correlations between ^{222}Rn and salinity ($r = 0.37$, $p < 0.10$) (Fig. 6). The ^{222}Rn observations do not allow distinguishing between inputs of fresh or saline SGD. When saline groundwater dominates SGD,

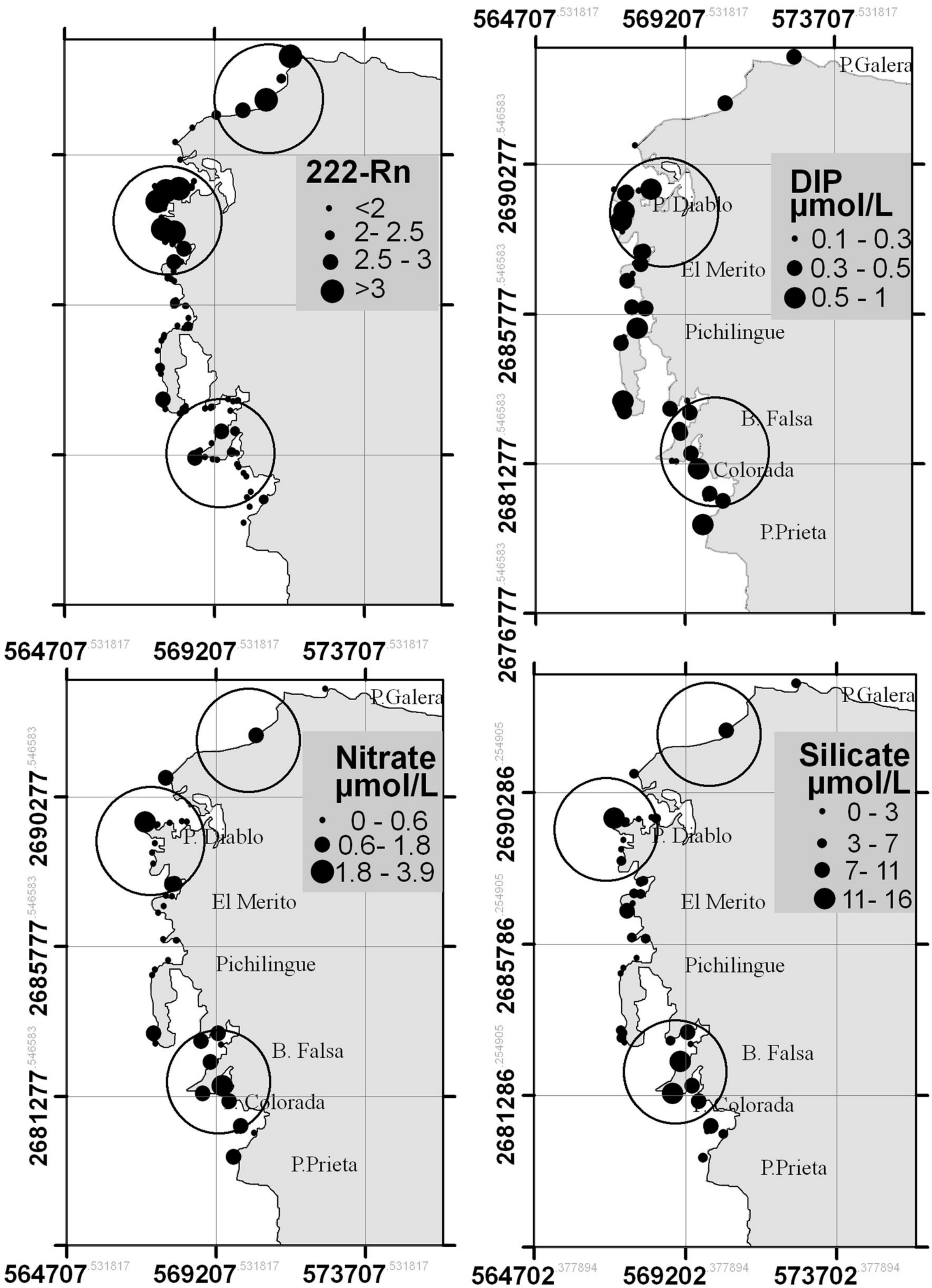

Fig. 4 Spatial distribution of nutrient concentrations and radon activities average from the four surveys. The *encircled areas* represent the hotspots for the different parameters

Table 2 Average ^{222}Rn activities and nutrient concentration in seawater during time series

Site	T °C	Salinity	^{222}Rn (dpm L^{-1})	NH_4 (μM)	NO_2 (μM)	NO_3 (μM)	SiO_2 (μM)	PO_4 (μM)
Balandra	27.8 ± 1.2	34.9 ± 0.1	1.4 ± 0.4	0.9 ± 0	nd	3.0 ± 2.7	14.4 ± 5.7	0.6 ± 0.7
Merito	21.2 ± 1.2	36.6 ± 0.3	1.2 ± 0.4	1.3 ± 0.3	0.2 ± 0.0	0.6 ± 3.5	12.1 ± 2.9	1.03 ± 0.2

n = 12 for Balandra and n = 24 for Merito

nd not detected

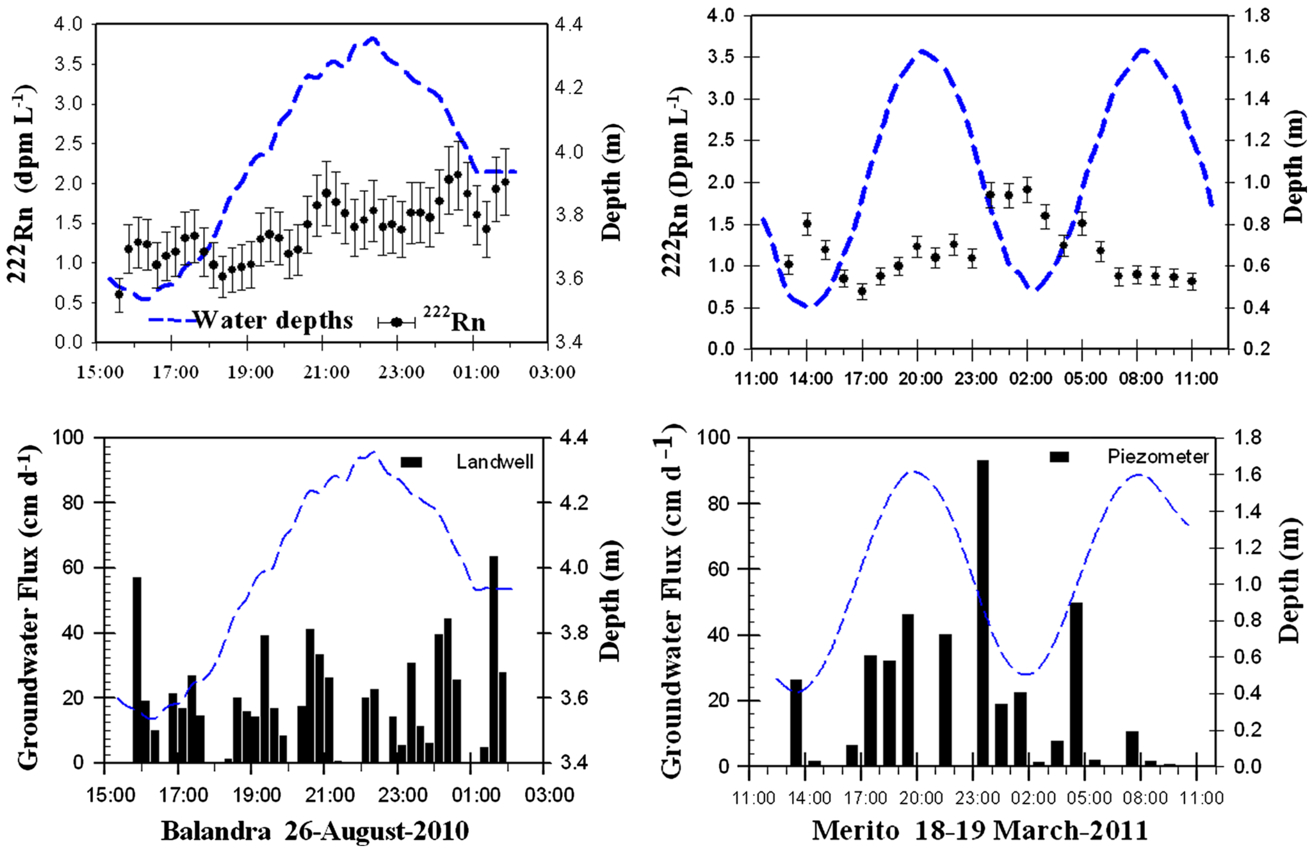

Fig. 5 Radon time series results (*left* Balandra; *right* Merito) and groundwater fluxes results from the mass model balance. The *dashed blue lines* represent water depths, the *dots* represent radon concentrations with *error bars* representing 2σ analytical uncertainties, and the *vertical bars* represent modeled groundwater discharge rates

unclear correlations may be expected between salinity and geochemical trace concentrations in surface waters (Boehm et al. 2006; Povinec et al. 2012; Street et al. 2008). A positive correlation between radon and salinity in Merito implies that saline recirculated water dominated SGD. In addition, the small but detectable pulse of freshwater was associated with relatively low radon concentrations (1.5 dpm L^{-1}) implying that saline SGD was more important than fresh groundwater as a source of radon. When assessing a large inverse estuary, Lamontagne et al. (2008) also obtained fresher water samples with low ^{222}Rn values in comparison to more saline samples. No correlations were found between radon and nutrients during the Merito experiment (Table 3). This site was located close to a mangrove area. Biogeochemical processes in mangroves effectively change the composition of groundwater and surface waters (Gleeson et al. 2013; Sanders et al. 2012). Mangroves effectively retain dissolved nutrients and have NH_4 as the dominant nitrogen species which may explain the lack of correlations between radon and nutrients in Merito (Table 3).

The Balandra site was relatively deeper (~4 m), 850 m away from the beach face, and along a rocky headland. ^{222}Rn increased during flood tide at Balandra, while salinity decreased following the behavior of an inverse estuary (Largier et al. 1997). The water within Balandra

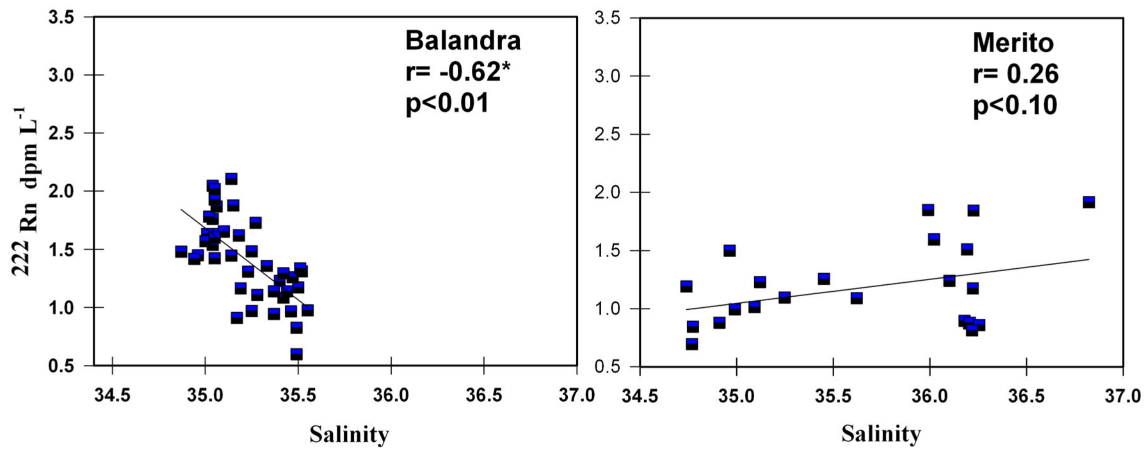

Fig. 6 Salinity versus radon in the time series of Balandra (*left*) and Merito (*right*)

Table 3 Correlations between radon and salinity versus nutrients in Balandra and Merito

	Water level	Salinity	NO_3	SiO_2	PO_4
Balandra					
^{222}Rn	$r = 0.56$*	$r = -0.62$*	$r = 0.84$*	$r = 0.80$*	$r = -0.11$
	$p < 0.05$	$p < 0.01$	$p < 0.05$	$p < 0.05$	$p > 0.10$
	$n = 42$	$n = 42$	$n = 12$	$n = 12$	$n = 12$
Salinity	$r = -0.69$*		$r = -0.63$*	$r = -0.48$	$r = 0.42$
	$p < 0.05$		$p < 0.05$	$p > 0.05$	$p > 0.10$
	$n = 42$		$n = 12$	$n = 12$	$n = 12$
Merito					
^{222}Rn	$r = -0.42$*	$r = 0.26$	$r = -0.14$	$r = -0.04$	$r = -0.09$
	$p < 0.05$	$p > 0.10$	$p > 0.10$	$p > 0.10$	$p > 0.10$
	$n = 23$	$n = 23$	$n = 23$	$n = 23$	$n = 23$
Salinity	$r = 0.09$		$r = -0.44$*	$r = 0.19$	$r = 0.25$
	$p > 0.10$		$p < 0.05$	$p > 0.10$	$p > 0.10$
	$n = 24$		$n = 24$	$n = 24$	$n = 24$

* Significant values

evaporates in the summer, causing salinity to be higher than the adjacent, deeper water body Bay of La Paz. Salinities registered during incoming tide oscillated between 34.4 and 34.8, slightly lower than the average salinity in the open La Paz Bay for September (35.09) and June (35.38) (Cervantes-Duarte et al. 2003). The high radon values at low salinities may suggest a signal of fresh SGD (Fig. 6). Significant positive correlations were found between radon and nitrates as well as silicates (Fig. 7) and no correlation with phosphates (Table 3). At other sites with major fresh groundwater inputs, significant correlations were found between groundwater tracers and inorganic nutrient concentrations in surface waters (Garrison et al. 2003; Santos et al. 2013; Street et al. 2008; Tait et al. 2014). In some cases silicates could be used as tracers of SGD (Kim et al. 2005). Silicate values oscillated between 6.17 and 22.6 µM which are higher than the open Bay of La Paz for summer (average 1.3 µM; Cervantes-Duarte et al. 2003) further implying active SGD at this site. The observed high nutrient values are unlikely to be driven by up-welling or remineralization. Previous studies showed that stratification is strongest in summer in La Paz Bay and that there was no evidence for mixing of surface and deep waters (Reyes-Salinas et al. 2003).

SGD rates and related nutrient fluxes

One of the main challenges in estimating SGD is defining ^{222}Rn and nutrient concentrations that represent the groundwater source (Dulaiova et al. 2008; Makings et al. 2014). We used a radon mass balance to estimate SGD rates based on one of two extreme assumptions: (1) the beach piezometer or (2) the inland well samples as the groundwater end-member as reported in Table 4. The different concentrations in those end-members result in different SGD estimates (Table 5).

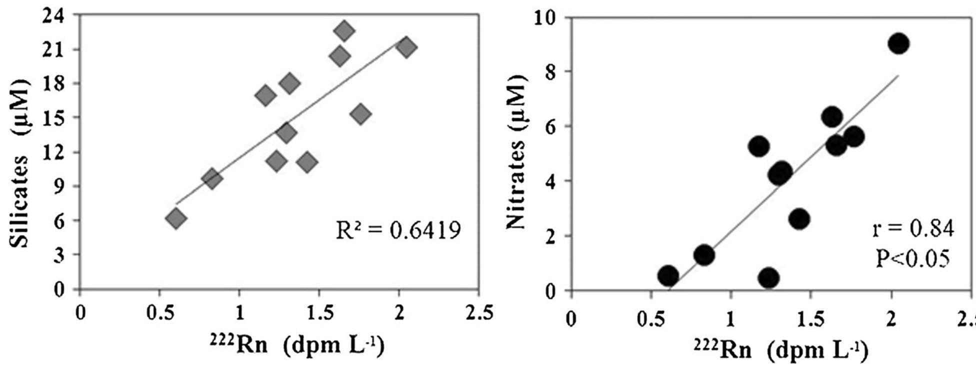

Fig. 7 Correlation between nitrate and silicate with ^{222}Rn during the Balandra time series. No correlations were found between radon and other nutrients

Table 4 ^{222}Rn and nutrient concentration (µM) in groundwater samples

Sample	Date	Longitude	Latitude	Depth	Salinity	Temp (°C)	^{222}Rn (dpm L^{-1})	NH_4 (µM)	NO_2 (µM)	NO_3 (µM)	SiO_2 (µM)	PO_4 (µM)
LW1	18-Oct-10	−110.262	24.2042	20 m	0.51	27.58	511	0.89	0.47	259	935	0.20
LW2	18-Oct-10	−110.251	24.2869	11 m	1.10	29.29	367	1.28	0.44	328	1060	0.22
Pz1	18-Mar-11	−110.327	24.3012	50 cm	37.48	22.14	Nd	2.61	1.01	7.36	29.6	5.18
Pz2	18-Mar-11	−110.327	24.3013	70 cm	37.37	22.0	33	14.8	0.21	6.02	44	5.61
Pz3	18-Mar-11	−110.326	24.3015	130 cm	34.28	19.8	25	4.42	0.2	10.14	39.6	4.9

Pzs beach piezometer, *LW* land wells

Table 5 Results of radon mass balance model and SGD fluxes using land wells and beach piezometer observations as the groundwater end-member

	Balandra		Merito	
	Land wells	Piezometer	Land wells	Piezometer
Water temperature (°C)	28.1 ± 0.7	28.1 ± 0.7	21.3 ± 1.3	21.3 ± 1.3
Salinity (UPS)	35.2 ± 0.2	35.2 ± 0.2	35.7 ± 0.6	35.7 ± 0.6
Wind speed (m s^{-1})	2.2 ± 1.1	2.2 ± 1.1	2.2 ± 0.9	2.2 ± 0.9
^{222}Rn (dpm L^{-1})	1.4 ± 0.4	1.4 ± 0.4	1.2 ± 0.1	1.2 ± 0.1
^{222}Rn mixing flux (dpm m^{-2} h^{-1})	−478/+115	−490/+115	−529/+100	−529/+103
^{222}Rn atmospheric flux (dpm m^{-2} h^{-1})	26 ± 13	27 ± 13	18 ± 9	18 ± 9
Total ^{222}Rn flux (dpm m^{-2} h^{-1})	3197 ± 674	3275 ± 688	221 ± 64	221 ± 64
Average SGD flux (cm day^{-1})	17.5 ± 4.2	267 ± 128	1.6 ± 0.4	18 ± 10

For Balandra, using the beach piezometer radon concentrations results in SGD fluxes that are unrealistic and too high at 267 cm day^{-1}. When using the inland well groundwater as an end-member, the SGD rates are more reasonable at 17.5 cm day^{-1} (Table 4) which is similar to the range estimated for the nearby Conception Bay (Santos et al. 2011) where hydrothermal springs occur. These high SGD rates may explain the significant correlations between silicates and nitrates with ^{222}Rn at Balandra. This also supports the suggestion that fresh rather than saline SGD dominates total SGD at Balandra. The Balandra time series was conducted 850 m off the beach face, and most SGD is expected to take place within about 100 m from the high-tide water mark (Burnett et al. 2006; Dulaiova et al. 2010). A complex and heterogenous aquifer with a deeper confined unit could explain SGD away from the shoreline (Bratton 2010). The local deep aquifer is heterogenous and complex (Sevilla-Unda 1994) and potentially extends to the zone where the radon time series was carried out (Fig. 8). The local geomorphology may also play a role as Balandra is located along a 360-m-high hill with a 30° slope. Higher fresh SGD is expected in sites located near to elevations such as headlands and cliffs in comparison to fluxes through beach face adjacent to low-lying areas (Mulligan and Charette 2006). The terrestrial topography exerts significant control due to local hydraulic gradients.

At Merito, a different process was observed. This site is shallow (2 m) and surrounded by intertidal sediments that become exposed during low tide. Porewater convection can occur when sediments are emerged and heated at low tide

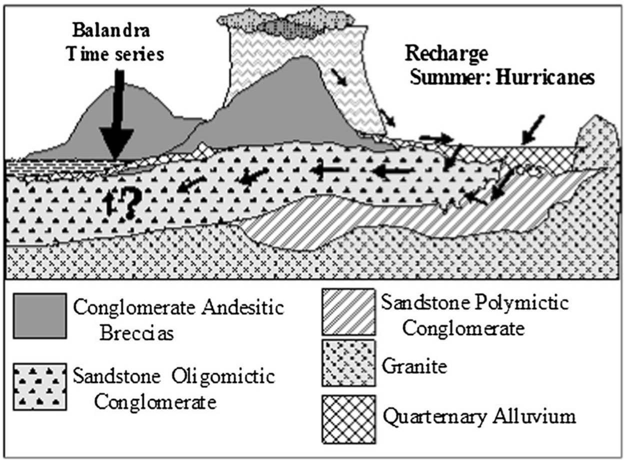

Fig. 8 Hydrogeologic conceptual model for the study site

(Rocha 2000). During the flood tide, colder seawater may create a sharp density gradient that may result in rapid shallow groundwater exchange. Convection can drive saline as well as a fresh SGD. This is consistent with the SGD fluxes calculated for Merito using boreholes values as the end-member which ranged from 0.6 to 93 cm day^{-1}, and may explain higher radon associated to higher salinities (Fig. 6).

SGD-derived nutrient fluxes were estimated by multiplying the radon-derived SGD rate by the nutrient concentration in the groundwater end-member (Table 6). Our results imply that there was a major component of shallow saline SGD at Merito. We thus opted for the use of shallow intertidal groundwater nutrient concentrations to estimate SGD-derived fluxes. In contrast, because Balandra was apparently dominated by fresh SGD, we used the groundwater from land wells that had higher nutrient concentrations. To extrapolate the advection rates to volumetric SGD and related nutrient fluxes, we assume that the ^{222}Rn time series integrated SGD inputs occurring within ~100 m from shore following Santos et al. (2011). Since the bay has a perimeter of 14.55 km, the seepage face was assumed to be 1.455 km^2. The average from Merito and Balandra results in an SGD flux of 9.6 cm day^{-1} (0.96 m^3 m^{-2} day^{-1}; Table 4) and a total SGD input of 1.61 m^3 s^{-1} for the seepage area of 1.45 km^2. Even using the most conservative scenario, and assuming a large saline SGD component, our estimates imply that this shallow coastal bay has rapid groundwater–surface water exchange rates. The estimated SGD-derived nutrient fluxes are within the broad range estimated in other similar investigations (Table 6).

The potential contribution of SGD-derived nutrient inputs to the productivity of the nearshore environment was explored using Redfield's ratio C:N of 6.6. We assumed that N was the limiting nutrient in the water column since N:P ratios were well below 16 (Table 2). The estimated dissolved inorganic nitrogen fluxes ($NH_4 + NO_3 + NO_2$; Table 6) can sustain primary productivity at rates ranging from 7 to 25 mg of C m^{-2} h. These estimates can be compared to reported primary productivity values for this region. Although pelagic primary productivity in the bay of La Paz can be highly variable seasonally (16–347 mg C m^{-2} h^{-1}) the most frequent values are between 42 and 125 mg of C m^{-2} h^{-1} (Reyes-Salinas et al. 2003). Therefore, SGD-derived dissolved inorganic nitrogen fluxes reported here can sustain 5–20 % of the reported regional primary productivity estimates. Our SGD estimates likely represent minimum contributions to productivity because we are able to quantify fluxes only in the summer when the time series experiments were performed. However, the highest radon and nitrogen concentrations

Table 6 SGD-derived nutrient fluxes compared to other arid or semi-arid locations

Site	SGD (m^3 m^{-2} day^{-1})	DIN (mmol m^{-2} day^{-1})	DIP (mmol m^{-2} day^{-1})	SiO_4 (mmol m^{-2} day^{-1})	References
Eilat, Israel	0.6–0.26	2.9–10	0.02–2.0	–	Shellenbarger et al. (2006)
Huntington Beach, USA	0.06–0.92	0.7–12	0.04–0.54	–	Boehm et al. (2004)
Jeju, South Korea	0.44	21.4	0.16	–	Hwang et al. (2005)
North Inlet, USA	0.3	2.42	0.91	–	Krest et al. (2000)
Pettaquamscutt, USA	0.002–0.02	0.17–0.49	0.01–0.04	–	Kelly and Moran (2002)
Spencer Beach, Hawaii	0.12–0.17	3.3–4.4	0.11–0.15	–	Street et al. (2008)
Kapauaiwa, Hawaii	0.37–0.39	6.8–7.0	0.42–0.45	–	Street et al. (2008)
Mahinahina, Hawaii	0.7–0.20	13–37	0.06–0.18	–	Street et al. (2008)
Average	0.10–0.18	1.5–28.2	0.02–0.93	6.7–95.3	This study
Balandra, Mexico	0.18	2.07–51.6	0.04–0.92	6.6–174.6	This study
Merito, Mexico	0.02–0.18	2.13–4.72	0.003–0.94	6.8–16	This study

The data range for Balandra and Merito rely on groundwater end-members obtained from shallow intertidal groundwaters, while the upper range boundary is given from results using data from land wells were found during the winter surveys likely as a result of SGD lagging precipitation events in the catchment.

Conclusions

Radon hotspots identified SGD sites along the southeast portion of La Paz Bay. The radon signal was stronger during winter than summer following a 3–4-month lag after the main rainfall events of the year. The two SGD hotspots appeared to be dominated by difference process. While Balandra was apparently dominated by fresh SGD, Merito was dominated by water recirculated in the shallow sediments. The estimated SGD rates of 0.18 and 0.96 m^3 m^{-2} day^{-1}, respectively, were comparable with data obtained in other arid and semi-arid places and were related to new nutrients fluxes that can explain between 5 and 20 % of the primary productivity values of La Paz Bay. If the SGD-derived nutrients are recycled within the water column, the SGD contribution to primary production could be much larger than estimated here. Overall, this study supports early investigations demonstrating that SGD can represent a major source of dissolved nutrients to arid environments. Considering the rainfall–SGD time lags implied from our observations and different driving forces at two nearby locations, long-term seasonal investigations covering episodic events are necessary to provide further insight into how SGD drives nutrient dynamics in arid systems.

Acknowledgments The authors thank Miguel Angel Juarez, Juan José Ramirez and Ivan Castro who provided valuable help in the field. Mexico's Consejo Nacional de Ciencia y Tecnología (CONACYT) financially supported this research and MU's Master's Thesis from which this paper has been derived (Project Grant 49815 and Scholarship Grant 337213). IRS acknowledges support from the Australian Research Council (DP120101645).

References

Aranda-Cirerol N, Herrera-Silveira JA, Comin FA (2006) Nutrient water quality in a tropical coastal zone with groundwater discharge, northwest Yucatan, Mexico. Estuar Coast Shelf Sci 68:445–454

Aranda-Gómez JJ (1982) El basamento metamórfico en la región de Todos Santos, B.C.S. Informe preliminar, México. DF Soc Geol Mexicana Convención Nacional Programa y Resúmenes, pp 103–104

Boehm AB, Paytan A, Shellenbarger GG, Davis KA (2006) Composition and flux of groundwater from a California beach aquifer: implications for nutrient supply to the surf zone. Cont Shelf Res 26:269–282

Boehm AB, Shellenbarger GG, Paytan A (2004) Groundwater discharge: potential association with fecal indicator bacteria in the surf zone. Environ Sci Technol 38:3558–3566

Bratton JF (2010) The three scales of submarine groundwater flow and discharge across passive continental margins. J Geol 118:565–575

Burnett WC, Dulaiova H (2003) Estimating the dynamics of groundwater input into the coastal zone via continuous radon-222 measurements. J Environ Radioact 69:21–35

Burnett W, Bokuniewicz H, Huettel M, Moore WS, Taniguchi M (2003) Groundwater and pore water inputs to the coastal zone. Biogeochemistry 66:3–33

Burnett WC, Aggarwal PK, Aureli A, Bokuniewicz H, Cable JE, Charette MA, Kontar E, Krupa S, Kulkarni KM, Loveless A, Moore WS, Oberdorfer JA, Oliveira J, Ozyurt IN, Povinec P, Privitera AMG, Rajar R, Ramessur RT, Schollten J, Stieglitz T, Taniguchi M, Turner JV (2006) Quantifying submarine groundwater discharge in the coastal zone via multiple methods. Sci Total Environ 367:498–543

Cervantes-Duarte R, Reyes-Salinas A, Verdugo-Diaz G, Valdez-Holguín JE (2003) Efecto de la concentración de clorofila a y seston superficial sobre la transparencia del agua de mar en una región costera del Golfo de California, México. Oceánides 18:1–11

Chávez-López S (2010) Hidrología de la Reserva de la Biosfera del Vizcaíno, B.C.S. In: Beltrán Morales LF, Chávez López S, Ortega Rubio A (eds) Valoración Hidrosocial en la Reserva de la Biosfera del Vizcaíno, B C S; México. CIBNOR, La Paz, Mexico, pp 35–52

Cruz-Orozco R, Martinez-Noriega C, Mendoza-Maravilla A (1996) Batimetría y sedimentos de la Bahía de La Paz, B.C.S., México. Oceánide 11:21–27

Dulaiova H, Peterson R, Burnett W, Lane-Smith D (2005) A multi-detector continuous monitor for assessment of ^{222}Rn in the coastal ocean. J Radioanal Nucl Chem 263:361–365

Dulaiova H, Gonneea ME, Henderson PB, Charette MA (2008) Geochemical and physical sources of radon variation in a subterranean estuary—implications for groundwater radon activities in submarine groundwater discharge studies. Mar Chem 110:120–127

Dulaiova H, Camilli R, Henderson PB, Charette MA (2010) Coupled radon, methane and nitrate sensors for large-scale assessment of groundwater discharge and non-point source pollution to coastal waters. J Environ Radioact 101:553–563

Garrison GH, Glenn CR, McMurtry GM (2003) Measurement of submarine groundwater discharge in Kahana Bay, O'ahu, Hawaii. Limnol Oceanogr 48:920–928

Gleeson J, Santos IR, Maher DT, Golsby-Smith L (2013) Groundwater–surface water exchange in a mangrove tidal creek: evidence from natural geochemical tracers and implications for nutrient budgets. Mar Chem 156:27–37. doi:10.1016/j.marchem.2013.02.001

Herrera-Silveira JA (1998) Nutrient–phytoplankton production relationships in a groundwater-influenced tropical coastal lagoon. Aquat Ecosyst Health Manag 1:373–385

Hwang DW, Lee YW, Kim G (2005) Large submarine groundwater discharge and benthic eutrophication in Bangdu Bay on volcanic Jeju Island, Korea. Limnol Oceanogr 50:1393–1403

Johannes RE (1980) The ecological significance of the submarine groundwater discharge. Mar Ecol Prog Ser 3:365–373

Kelly RP, Moran SB (2002) Seasonal changes in groundwater input to a well-mixed estuary estimated using radium isotopes and implications for coastal nutrient budgets. Limnol Oceanogr 47:1807–1976

Kim G, Ryu JW, Yang HS, Yun ST (2005) Submarine groundwater discharge (SGD) into the Yellow Sea revealed by Ra-228 and Ra-226 isotopes: implications for global silicate fluxes. Earth Planet Sci Lett 237:156–166

Krest JM, Moore WS, Gardner RL, Morris JT (2000) Marsh Nutrient supplied by groundwater discharge: evidence from radium measurements. Glob Biogeochem Cycles 14:36-47. doi:10.1029/1999GB001197

Kroeger KD, Charette MA (2008) Nitrogen biogeochemistry of submarine groundwater discharge. Limnol Oceanogr 53:1025–1039

Lamontagne S, Le Gal La Salle C, Hancock GJ, Webster IT, Simmons CT, Love AJ, James-Smith J, Smith AJ, Kämpf J, Fallowfield HJ (2008) Radium and radon radioisotopes in regional groundwater, intertidal groundwater, and seawater in the Adelaide Coastal Waters Study area: implications for the evaluation of submarine groundwater discharge. Mar Chem 109:318–336

Largier JL, Hollibaugh JT, Smith SV (1997) Seasonally hypersaline estuaries in Mediterranean-climate regions. Estuar Coast Shelf Sci 47:789–797

Macklin PA, Maher DT, Santos IR (2014) Estuarine canal estate waters: hotspots of CO_2 outgassing driven by enhanced groundwater discharge? Mar Chem 167:82–92. doi:10.1016/j.marchem.2014.08.002

Makings U, Santos IR, Maher DT, Golsby-Smith L, Eyre BD (2014) Importance of budgets for estimating the input of groundwater-derived nutrients to an eutrophic tidal river and estuary. Estuar Coast Shelf Sci 143:65–76. doi:10.1016/j.ecss.2014.02.003

Mendoza-Salgado RA, Lechuga-Deveze CH, Ortega-Rubio A (2006) Influence of rainfall on a subtropical arid zone coastal system. J Arid Environ 66:247–256

Michael HA, Mulligan AE, Harvey CF (2005) Seasonal oscillations in water exchange between aquifers and the coastal ocean. Nature 436:1145–1148

Moore WS (1997) High fluxes of radium and barium from the mouth of the Ganges-Brahmaputra River during low river discharge suggest a large groundwater source. Earth Planet Sci Lett 150:141–150

Moore WS (2010) The effect of submarine groundwater discharge on the ocean. Ann Rev Mar Sci 2:59–88

Mulligan AE, Charette MA (2006) Intercomparison of submarine groundwater discharge estimates from a sandy unconfined aquifer. J Hydrol 327:411–425

Niencheski LFH, Windom HL, Moore WS, Jahnke RA (2007) Submarine groundwater discharge of nutrients to the ocean along a coastal lagoon barrier, Southern Brazil. Mar Chem 106:546–561

Perkins AK, Santos IR, Sadat-Noori M, Gatland JR, Maher DT (2015) Groundwater seepage as a driver of CO_2 evasion in a coastal lake (Lake Ainsworth, NSW, Australia). Environ Earth Sci 1–14. doi:10.1007/s12665-015-4082-7

Peterson RN, Burnett WC, Dimova N, Santos IR (2009) Comparison of measurement methods for radium-226 on manganese-fiber. Limnol Oceanogr Methods 7:196–205

Povinec PP, Burnett WC, Beck A, Bokuniewicz H, Charette M, Gonneea ME, Groening M, Ishitobi T, Kontar E, Liong Wee Kwong L, Marie DEP, Moore WS, Oberdorfer JA, Peterson R, Ramessur R, Rapaglia J, Stieglitz T, Top Z (2012) Isotopic, geophysical and biogeochemical investigation of submarine groundwater discharge: IAEA-UNESCO intercomparison exercise at Mauritius Island. J Environ Radioact 104:24–45

Reyes-Salinas A, Cervantes-Duarte R, Morales-Pérez RA, Valdez-Holguín JE (2003) Variabilidad estacional de la productividad primaria y su relación con la estratificación vertical en la bahía de la Paz, B.C.S. Hidrobiológica 13:103–110

Rocha C (2000) Density-driven convection during flooding of warm, permeable intertidal sediments: the ecological importance of the convective turnover pump. J Sea Res 43:1–14

Sanders CJ, Santos IR, Barcellos R, Silva Filho EV (2012) Elevated concentrations of dissolved Ba, Fe and Mn in a mangrove subterranean estuary: consequence of sea level rise? Cont Shelf Res 43:86–94. doi:10.1016/j.csr.2012.04.015

Santos IR, Lechuga-Deveze C, Peterson RN, Burnett WC (2011) Tracing submarine hydrothermal inputs into a coastal bay in Baja California using radon. Chem Geol 282:1–10

Santos IR, Cook PLM, Rogers L, de Weys J, Eyre BD (2012a) The 'salt wedge pump': convection-driven porewater exchange as a source of dissolved organic and inorganic carbon and nitrogen to an estuary. Limnol Oceanogr 57:1415–1426

Santos IR, Eyre BD, Huettel M (2012b) The driving forces of porewater and groundwater flow in permeable coastal sediments: a review. Estuar Coast Shelf Sci 98:1–15

Santos IR, de Weys J, Tait DR, Eyre BD (2013) The contribution of groundwater discharge to nutrient exports from a coastal catchment: post-flood seepage increases estuarine N/P ratios. Estuaries Coasts 36:56–73

Santos IR, Bryan KR, Pilditch CA, Tait DR (2014) Influence of porewater exchange on nutrient dynamics in two New Zealand estuarine intertidal flats. Mar Chem 167:57–70. doi:10.1016/j.marchem.2014.04.006

Santos IR, Beck M, Brumsack H-J, Maher DT, Dittmar T, Waska H, Schnetger B (2015) Porewater exchange as a driver of carbon dynamics across a terrestrial-marine transect: insights from coupled ^{222}Rn and pCO_2 observations in the German Wadden Sea. Mar Chem 171:10–20. doi:10.1016/j.marchem.2015.02.005

Schmidt A, Stringer CE, Haferkorn U, Schubert M (2008) Quantification of groundwater discharge into lakes using radon-222 as naturally occurring tracer. Environ Geol. doi:10.1007/s00254-00008-01186-00253

Schubert M, Paschke A, Lieberman E, Burnett WC (2012) Air–water partitioning of ^{222}Rn and its dependence on water temperature and salinity. Environ Sci Technol 46:3905–3911

Sedlock RL, Ortega-Gutiérrez F, Speed RC (1993) Tectono-stratigraphic terrenes and tectonic evolution of Mexico. Geol Soc Am Spec Pap 278:153

Sevilla-Unda VE (1994) Reconocimiento Hidrogeológico del Valle el Coyote, Baja California Sur. México. Tesis de Licenciatura. Universidad Autónoma de Baja California Sur. pp 101

Shellenbarger GG, Monismith SG, Genin A, Paytan A (2006) The importance of submarine groundwater discharge to the nearshore nutrient supply in the Gulf of Aqaba (Israel). Limnol Oceanogr 51:1876–1886

Slomp CP, Van Cappellen P (2004) Nutrient inputs to the coastal ocean through submarine groundwater discharge: controls and potential impact. J Hydrol 295:64–86

Stieglitz TC, Cook PG, Burnett WC (2010) Inferring coastal processes from regional-scale mapping of ^{222}Radon and salinity: examples from the Great Barrier Reef, Australia. J Environ Radioact 101:544–552

Street JH, Knee KL, Grossman EE, Paytan A (2008) Submarine groundwater discharge and nutrient addition to the coastal zone and coral reefs of leeward Hawai'i. Mar Chem 109:355–376

Strickland JHD, Parsons T (1972) A practical handbook of seawater analysis, 2nd edn. Fisheries Research Board of Canada Bulletin, Ottawa

Swarzenski PW, Burnett WC, Greenwood WJ, Herut B, Peterson R, Dimova N, Shalem Y, Yechieli Y, Weinstein Y (2006) Combined time-series resistivity and geochemical tracer techniques to examine submarine groundwater discharge at Dor Beach, Israel. Geophys Res Lett 33:L24405. doi:10.1029/2006GL028282

Tait DR, Erler DV, Santos IR, Cyronak TJ, Morgenstern U, Eyre BD (2014) The influence of groundwater inputs and age on nutrient dynamics in a coral reef lagoon. Mar Chem 166:36–47. doi:10.1016/j.marchem.2014.08.004

Valiela I, Costa J, Foreman K, Teal JM, Howes B, Aubrey D (1990) Transport of groundwater-borne nutrients from watersheds and their effects on coastal waters. Biogeochemistry 10:177–197

Velasco-García JA (2009) Ambientes Geológicos Costeros del Litoral de la Bahía de la Paz. Baja California Sur, Mexico

Waska H, Kim G (2010) Differences in microphytobenthos and macrofaunal abundances associated with groundwater discharge in the intertidal zone. Mar Ecol Prog Ser 407:159–172

Waska H, Kim S, Kim G, Peterson RN, Burnett WC (2008) An efficient and simple method for measuring ^{226}Ra using the scintillation cell in a delayed coincidence counting system (RaDeCC). J Environ Radioact 99:1859–1862

Weinstein Y, Burnett WC, Swarzenski PW, Shalem Y, Yechieli Y, Herut B (2007) Role of aquifer heterogeneity in fresh groundwater discharge and seawater recycling: An example from the Carmel Coast, Israel. J Geophys Res 112:C12016. doi:10.1029/2007JC004112

Young MB, Gonneea ME, Fong DA, Moore WS, Herrera-Silveira J, Paytan A (2008) Characterizing sources of groundwater to a tropical coastal lagoon in a karstic area using radium isotopes and water chemistry. Mar Chem 109:377–394